



Crystal Structure of the Agrin-responsive Immunoglobulin-like Domains 1 and 2 of the Receptor Tyrosine Kinase MuSK

Amy L. Stiegler¹, Steven J. Burden² and Stevan R. Hubbard^{1*}

¹Structural Biology Program
Skirball Institute of
Biomolecular Medicine and
Department of Pharmacology
New York University School
of Medicine, New York
NY 10016, USA

²Molecular Neurobiology
Program, Skirball Institute
of Biomolecular Medicine
New York University School of
Medicine, New York
NY 10016, USA

Muscle-specific kinase (MuSK) is a receptor tyrosine kinase expressed exclusively in skeletal muscle, where it is required for formation of the neuromuscular junction. MuSK is activated by agrin, a neuron-derived heparan sulfate proteoglycan. Here, we report the crystal structure of the agrin-responsive first and second immunoglobulin-like domains (Ig1 and Ig2) of the MuSK ectodomain at 2.2 Å resolution. The structure reveals that MuSK Ig1 and Ig2 are Ig-like domains of the I-set subfamily, which are configured in a linear, semi-rigid arrangement. In addition to the canonical internal disulfide bridge, Ig1 contains a second, solvent-exposed disulfide bridge, which our biochemical data indicate is critical for proper folding of Ig1 and processing of MuSK. Two Ig1-2 molecules form a non-crystallographic dimer that is mediated by a unique hydrophobic patch on the surface of Ig1. Biochemical analyses of MuSK mutants introduced into MuSK^{-/-} myotubes demonstrate that residues in this hydrophobic patch are critical for agrin-induced MuSK activation.

© 2006 Elsevier Ltd. All rights reserved.

Keywords: agrin; crystal structure; MuSK; neuromuscular junction; receptor tyrosine kinase

*Corresponding author

Introduction

Formation of the vertebrate neuromuscular junction is guided by the exchange of signals between innervating motor neurons and muscle cells, resulting in a highly specialized postsynaptic membrane and differentiated nerve terminal, which are spatially juxtaposed.¹ Neuromuscular synapse formation depends upon agrin, a large (>200 kDa), multidomain heparan sulfate proteoglycan that is secreted by motor axons and becomes stably localized in the synaptic basal lamina.² Agrin stimulates postsynaptic differentiation by activating the muscle-specific kinase (MuSK), a receptor tyrosine kinase (RTK) expressed exclusively in skeletal muscle.^{3–5} Agrin and MuSK are critical

for proper synaptic development, as both agrin-deficient and MuSK-deficient mice lack mature neuromuscular junctions and consequently die at birth due to a failure to breathe.^{6,7} Downstream of agrin-induced MuSK activation, muscle-derived proteins including acetylcholine receptors (AChRs), rapsyn, ErbBs, and MuSK itself, are redistributed to the postsynaptic site and become stably localized in clusters beneath the nerve terminal.^{6,8} In addition, agrin-induced MuSK activation leads to selective transcriptional upregulation of synapse-specific genes by subsynaptic nuclei, and to induction of a retrograde signal leading to presynaptic differentiation.⁶

Other members of the RTK family include the receptors for growth factors such as the fibroblast growth factors (FGFs), vascular endothelial growth factor, epidermal growth factor and nerve growth factor (NGF). Typically, an RTK is activated through direct binding of its cognate ligand to the receptor ectodomain, which induces receptor dimerization (or higher-order oligomerization) and *trans*-autophosphorylation of tyrosine residues in the cytoplasmic, tyrosine kinase-containing domain.^{9,10}

Unlike other ligand–RTK pairs, a direct interaction between agrin and the MuSK ectodomain has not

Abbreviations used: MuSK, muscle-specific kinase; RTK, receptor tyrosine kinase; AChR, acetylcholine receptor; FGF, fibroblast growth factor; NGF, nerve growth factor; GFP, green fluorescent protein; FBS, fetal bovine serum.

E-mail address of the corresponding author:
hubbard@saturn.med.nyu.edu

been demonstrated.⁵ On the basis of several observations, however, agrin is still regarded as the ligand for MuSK. First, agrin stimulates the phosphorylation and kinase activity of MuSK in cultured myotubes with kinetics characteristic of ligand–receptor pairs.⁵ Second, cultured muscle cells lacking MuSK and cells expressing a kinase-dead/dominant-negative mutant MuSK are unable to form AChR clusters in response to treatment with agrin.^{5,11} Lastly, agrin-deficient and MuSK-deficient mice have very similar phenotypes.^{6,7} Despite such evidence supporting MuSK as the receptor for agrin, the failure to demonstrate a direct interaction between the two proteins has raised the possibility that an additional myotube-associated specificity component, such as a co-ligand, co-receptor, or myotube-specific post-translational modification, is required for agrin to bind and activate MuSK.⁵ This hypothesis is supported by the observation that when MuSK is ectopically expressed in fibroblasts or myoblasts, treatment with agrin fails to stimulate MuSK phosphorylation.⁵

The ectodomain of MuSK comprises four globular domains: three N-terminal immunoglobulin-like (Ig) domains,^{3,4} and a C-terminal cysteine-rich region similar to the cysteine-rich domain of Frizzled, the receptor for Wnt.^{12,13} Ig-like domains in other RTKs, including FGF receptors, TrkA (NGF receptor), and vascular endothelial growth factor receptor-1, serve as the ligand-binding site.¹⁴ Earlier studies aimed at identifying the domains within the MuSK ectodomain that are critical for agrin-induced AChR clustering demonstrated that the first and second Ig-like domains (Ig1 and Ig2) of MuSK are sufficient to rescue AChR clustering in MuSK^{−/−} myotubes, suggesting that the binding site for agrin and/or the putative co-receptor resides within these two domains of MuSK.¹⁵

The lack of a direct interaction between agrin and MuSK *in vitro* (data not shown),⁵ along with the dependence on multiple domains of agrin for MuSK activation⁸ and maximal AChR clustering,^{16–18} makes co-crystallization of agrin with the MuSK ectodomain problematic. Therefore, in an attempt to gain insights into the mechanism by which MuSK is activated by agrin, we have determined the crystal structure of Ig1-2 from the MuSK ectodomain alone. Our structural and biochemical data reveal that Ig1 possesses unique properties that are important for responsiveness to agrin and for receptor processing.

Results and Discussion

Crystal structure of MuSK Ig1-2

Ig1-2 of the rat MuSK ectodomain was expressed in a baculovirus/insect cell system. Crystals were obtained in space group *P*2₁2₁2₁, with two Ig1-2 molecules in the asymmetric unit. The structure was determined by molecular replacement (see Materials and Methods) and refined at 2.2 Å resolution. Data

collection and refinement statistics are given in Table 1. The crystal structure reveals that both Ig1 and Ig2 belong to the intermediate set (I-set) of the immunoglobulin superfamily (Figure 1(a)).¹⁹ In I-set Ig-like domains, two anti-parallel β sheets, one containing four β strands (ABED) and the other containing five (A'GFCC'), are linked by an internal disulfide bridge between βB and βF, forming a β sandwich. The I-set is also characterized by a 20-residue sequence profile.¹⁹ MuSK Ig1 contains 18 of the 20 I-set profile residues (diverging at Glu42 and Gly113), while Ig2 contains all 20 residues.

Ig1 superimposes onto telokin (PDB code 1FHG),²⁰ its closest structural neighbor and prototypical I-set member, with a root-mean-square-deviation (r.m.s.d.) of 1.2 Å between equivalent C^α atoms (92 residues, 30% identity). The nearest structural neighbor to Ig2 is Ig4 of axonin-1 (PDB code 1CS6),²¹ with an r.m.s.d. of 1.3 Å for equivalent C^α atoms (89 residues, 31% identity). Also, Ig1 and Ig2 superimpose onto each other with an r.m.s.d. of 1.4 Å (90 residues, 29% identity).

An intriguing feature of MuSK Ig1 is the presence of a second disulfide bridge (in addition to the canonical internal disulfide bridge), which is on the surface of the domain and is formed by Cys98 and

Table 1. X-Ray data collection and refinement statistics

<i>Data collection</i>	
Resolution (Å)	50.0–2.20
Observations	98,037
Unique reflections	27,127
Completeness ^a (%)	98.7 (97.5)
<i>R</i> _{sym} ^{a,b} (%)	6.0 (33.1)
<i>I</i> / <i>σI</i>	15.9 (4.2)
<i>Refinement</i>	
Number of atoms	
Protein	2830
Water	178
Sulfate	15 (3 ions)
Resolution (Å)	30.0–2.20
Reflections	24,821
<i>R</i> _{cryst} ^c (%)	21.6
<i>R</i> _{free} ^c (%)	25.8
rmsd values	
Bond lengths (Å)	0.010
Bond angles (deg.)	1.3
<i>B</i> -factors ^d (Å ²) (backbone/side-chain)	0.75/1.73
Average <i>B</i> -factors (Å ²)	
All atoms	31.9
Protein	31.9
Water	31.1
Sulfate	40.8
Ramachandran plot statistics	
Most favored regions (%)	89.5
Additionally allowed regions (%)	10.5
Generously allowed regions (%)	0
Disallowed regions (%)	0

^a The overall value is given first, with the value in the highest resolution shell (2.28–2.20 Å) given in parentheses.

^b $R_{\text{sym}} = 100 \sum |I - \langle I \rangle| / \sum I$.

^c $R_{\text{cryst}} = 100 \sum ||F_o| - |F_c|| / \sum |F_o|$, where *F*_o and *F*_c are the observed and calculated structure factors, respectively (*F*_o > 0 *σ*). *R*_{free} was determined from ~5% of the data (1309 reflections).

^d For bonded atoms.

Cys112 on neighboring strands β F and β G (Figures 1(a) and 2(c), right). Cysteine residues at these positions in an Ig-like domain are unique to MuSK Ig1 (see Figure 1(c) for alignment), yet are conserved in MuSK from *Torpedo californica* to human, reflect-

ing their potential functional importance. An exposed cross-strand disulfide bridge at the same position is found also in fibronectin type III domains (which are topologically similar to Ig-like domains) in class 2 cytokine receptors, including interferon

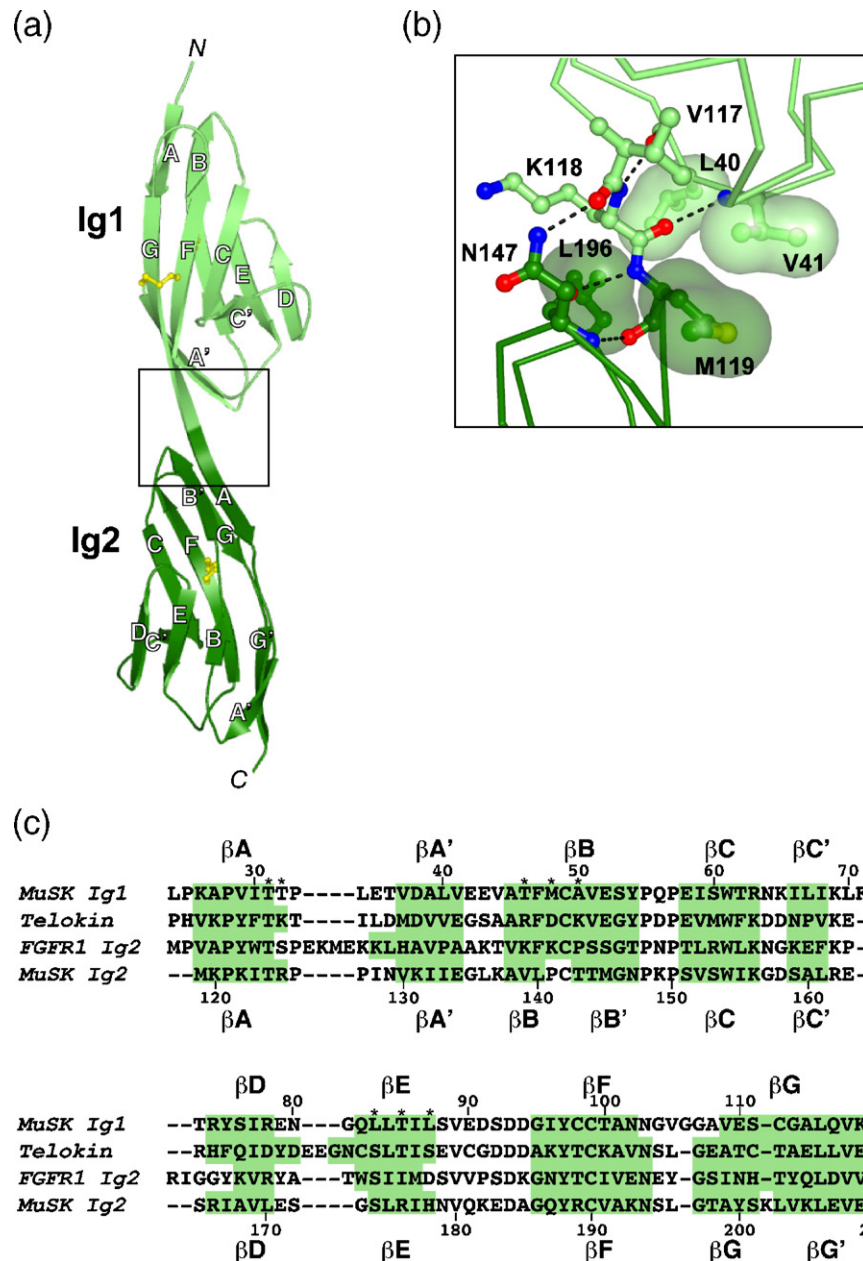


Figure 1. Crystal structure of MuSK Ig1-2. (a) Ribbon diagram of MuSK Ig1-2. Ig1 is colored light green and Ig2 is colored dark green. The β strands are labeled, as are the N and C termini (N and C, respectively). Cysteine side-chains are shown in ball-and-stick representation and are colored yellow. The box indicates the region highlighted in (b), which shows the Ig1-Ig2 domain interface. Residues involved in interdomain contacts are shown in stick representation on top of a C^α trace. Oxygen atoms, red; nitrogen atoms, blue; sulfur atoms, yellow; and carbon atoms, light green (Ig1) or dark green (Ig2). Hydrogen bonds are depicted as broken black lines. The van der Waals surfaces (semi-transparent) are shown for selected side-chains. (c) Structure-based sequence alignment of select I-set Ig-like domains showing the sequences for MuSK Ig1 and Ig2 (rat), telokin (turkey, PDB code 1FHG),²⁰ and FGFR1 domain 2 (human, PDB code 1CVS).⁴² Structural alignment was achieved using Dali.⁴³ Residues in β strands, as determined by PROCHECK,⁴⁴ are highlighted in green, and the identity of each strand is indicated above and below the sequences. Residue numbering is for MuSK Ig1 (above) and Ig2 (below), with every tenth residue numbered. Residues located in the Ig1-mediated dimer interface are marked with an asterisk (*). The V-frame nomenclature used in the text derives from Harpaz and Chothia.¹⁹ For example, residue A'B1 is the first residue in the A'B loop, and G6 is the sixth residue in β G. (a) and (b) were rendered with PyMOL [<http://pymol.sourceforge.net>].

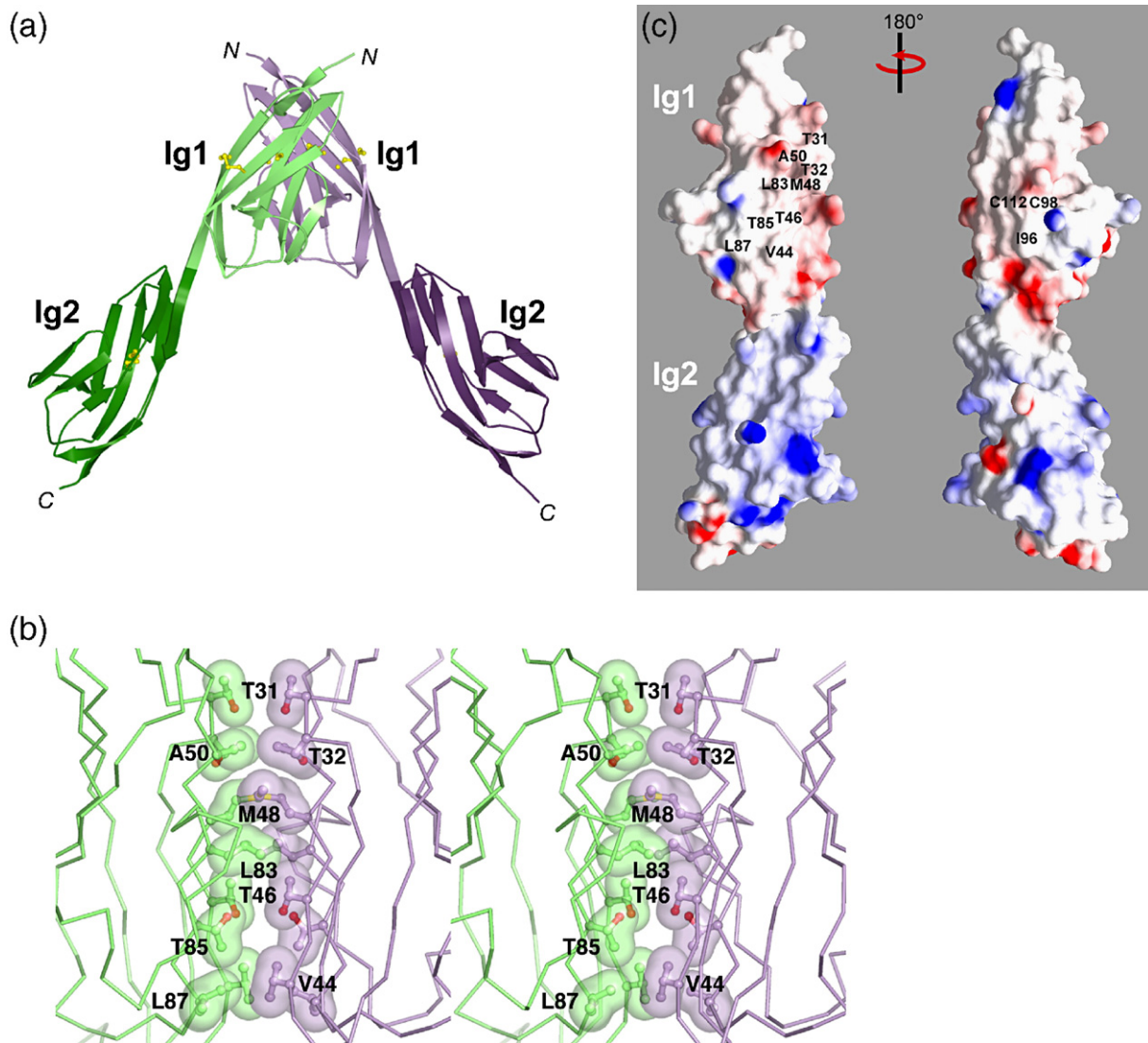


Figure 2. MuSK Ig1-2 dimer. (a) Ribbon diagram of the MuSK Ig1-2 non-crystallographic dimer. The two protomers are colored green and purple (Ig1 in light shades and Ig2 in dark shades). The non-crystallographic 2-fold axis is vertical. (b) Ig1-Ig1 dimer interface. The stereo view is approximately 50° about the vertical (2-fold) axis from that in (a). Side-chain atoms in the dimer interface are shown in ball-and-stick representation, and hydrophobic contacts are shown with semi-transparent van der Waals surfaces. Carbon atoms, either green or purple; oxygen atoms, red; and sulfur atoms, yellow. Side-chains that are not labeled are related by the vertical 2-fold axis to those that are labeled. (c) Molecular surface representation of Ig1-2 colored according to electrostatic potential: blue, positive (+15kT); white, neutral; red, negative (−15kT). Residues located in the Ig1 dimer interface (left) and in the vicinity of the surface-exposed disulfide bridge (Cys98/Cys112) (right), on the opposite side of Ig1, are labeled. The two views are related by 180° about a vertical axis. (a) and (b) were rendered with PyMOL [<http://pymol.sourceforge.net>] and (c) with GRASP.⁴⁵

receptors and tissue factor.^{22–24} In MuSK Ig1, the cross-strand disulfide bridge does not affect the overall fold of Ig1, nor does it alter the local structure of β F and β G.

Ig1 and Ig2 are disposed in a linear, head-to-tail fashion, and abut to form a rod-like molecule (Figures 1(a) and 2(c)). There is no polypeptide linker between the two domains; the final strand of Ig1 (β G) is contiguous with the first strand of Ig2 (β A) (Figure 1(b)). Interdomain contacts are present between the bottom (C-terminal) end of Ig1 and the upper (N-terminal) end of Ig2, burying 416 Å² of surface area. The interface includes the side-chains of Leu40, Val41 in Ig1 and Met119, Leu196 in Ig2,

which make van der Waals contacts (Figure 1(b)). In addition, Asn147 in Ig2 forms a hydrogen bond with the carbonyl oxygen atom of Val117 in Ig1. These Ig1-Ig2 interface residues are conserved in MuSK from *Torpedo* to human. This interface presumably functions to preserve the linear arrangement of the two domains. On the basis of a sequence alignment of the MuSK Ig-like domains, we predict that Ig2 and Ig3 will also be contiguous, indicating that the first three domains of the MuSK ectodomain adopt a semi-rigid linear arrangement. It is noteworthy that a natural splice variant of MuSK contains an additional ten residues precisely at the Ig2-Ig3 junction,^{4,25} which would likely introduce greater

flexibility into the MuSK ectodomain, but the function of this splice insert is not known.

In the crystal structure, a non-crystallographic dimer of Ig1-2 is present, which is mediated solely by residues in Ig1 (Figure 2(a)). The dimer interface is predominantly hydrophobic in nature, burying 1314 Å² of total surface area with a shape complementarity (*sc*) value of 0.58.²⁶ Met48 in βB and Leu83 in βE are at the center of the interface (Figure 2(b)). In a typical I-set Ig-like domain, the residues at these two positions are hydrophilic (e.g. Lys177 and Ser214, respectively, in FGF receptor-1, see Figure 1(c)), as they are solvent-exposed in a monomeric Ig-like domain (Figure 2(c), left). In MuSK, these two residues are well conserved from *Torpedo* to human (Met48 is replaced by valine in chicken MuSK, and Leu83 is replaced by isoleucine in *Torpedo* MuSK). Additional van der Waals contributions to the interface are made by Thr31 and Thr32 (AA' loop), Val44, Thr46 and Ala50 (βB), and Thr85 and Val87 (βE) (Figure 2(b)). Although there are no direct hydrogen bonds across the dimer interface, there are several water-mediated ones. A crystallographic dimer is present in the structure (1677 Å² of buried surface area, *sc* value of 0.58), with an Ig1-Ig2 interface, but this largely hydrophilic interface is not conserved in *Torpedo* MuSK. Size-exclusion chromatography indicates that soluble Ig1-2 is monomeric (up to a loading concentration of 180 μM; data not shown), although this does not preclude the possibility that MuSK forms a dimer on the cell surface, where the orientation and lateral mobility of the MuSK ectodomain will be restricted due to membrane anchoring.

The two copies of Ig1 in the asymmetric unit are very similar, with an r.m.s.d. value of 0.9 Å upon superposition of all 94 C^α atoms, and of only 0.4 Å when residues of the C'D loop (residues 69–72) are excluded. The two copies of Ig2 in the asymmetric unit are also very similar, and superimpose with an r.m.s.d. of 0.4 Å (92 C^α atoms). Comparison of the two copies of the intact Ig1-2 molecule in the asymmetric unit after superposition on Ig1 reveals that, despite the interdomain contacts described above, some flexibility is present, as the Ig2 domains in the Ig1 superposition are 22° apart, with the hinge point at Lys118 at the end of Ig1. The C termini of the Ig2 domains in the non-crystallographic dimer are ~80 Å apart.

Extra disulfide in MuSK Ig1 is required for proper folding of Ig1

The structure reveals that the additional pair of cysteine residues in MuSK Ig1 (Cys98 and Cys112) forms a surface-exposed disulfide bridge. A surface-exposed disulfide bridge is also found in Ig-like domain-5 of TrkA, and is located in a hydrophobic region that provides part of the binding site for its ligand, NGF.²⁷ To probe the function of the external disulfide bridge in MuSK Ig1, both Cys98 and Cys112 were mutated to serine (C98S/C112S) in a full-length MuSK-green fluorescent protein (GFP)

fusion construct, and wild-type or mutant MuSK-GFP was stably expressed by retroviral infection in NIH-3T3 fibroblasts and MuSK^{-/-} cultured muscle cells. We first tested whether MuSK C98S/C112S was expressed on the muscle cell surface. To this end, we labeled cell-surface proteins on cultured myotubes expressing wild-type or mutant MuSK C98S/C112S with water-soluble, membrane-impermeable NHS-activated biotin, which reacts with primary amines. After biotin-labeling, the cells were lysed and biotin-conjugated proteins isolated with streptavidin-agarose beads. Biotin-labeled and total proteins were separated by SDS-PAGE and transferred to polyvinylidene difluoride (PVDF) membranes. Probing Western blots with antibodies directed against cell-surface proteins such as the insulin receptor reveals that NHS-biotin effectively labels cell-surface proteins, while intracellular proteins such as Shc remain unlabeled (Figure 3(a)). Unlike the wild-type receptor, MuSK C98S/C112S fails to be labeled by biotin (Figure 3(a)). We therefore conclude that the mutant receptor C98S/C112S is not expressed on the cell surface.

The failure of MuSK C98S/C112S to be expressed on the cell surface could be a consequence of improper folding and/or processing of the receptor, leading to retention of the mutant receptor in the endoplasmic reticulum or Golgi. Consistent with this hypothesis, we observe that the majority of the MuSK C98S/C112S protein migrates faster in SDS-PAGE *versus* wild-type MuSK, which is likely due to incomplete or no N-linked glycosylation of the mutant receptor (Figure 3(b), see the anti-GFP blot of the lysates). It has been shown that deglycosylation of MuSK by chemical treatment or asparagine mutation causes the receptor to migrate faster in SDS-PAGE.²⁸ However, asparagine mutation of MuSK does not affect the ability of the unglycosylated receptor to be expressed on the cell surface, since the mutant receptors are activated by agrin. Therefore, it is probable that mutation of the surface-exposed disulfide bridge causes misfolding of Ig1, leading to retention of MuSK C98S/C112S inside the cell and subsequent underglycosylation of the mutant receptor. Since MuSK C98S/C112S is efficiently immunoprecipitated by an antibody against the N-terminal β strand of Ig1 (see below) and is recognized in an anti-GFP (C-terminal) immunoblot, we rule out the possibility that the change in migration of the mutant receptor on SDS-PAGE is due to proteolysis.

To assess whether removal of the additional disulfide bridge (Cys98 and Cys112) causes misfolding of Ig1, we tested the ability of a polyclonal antibody raised against a peptide encompassing the βA-βA' region of Ig1 (residues 20–39) to immunoprecipitate wild-type or mutant MuSK from lysates of NIH-3T3 cells and myotubes. We find that MuSK C98S/C112S, but not wild-type, can be immunoprecipitated efficiently from lysates of both cell types by this N-terminal polyclonal antibody (Figure 3(b) and data not shown), although both receptors are detected by this antibody by immunoblot

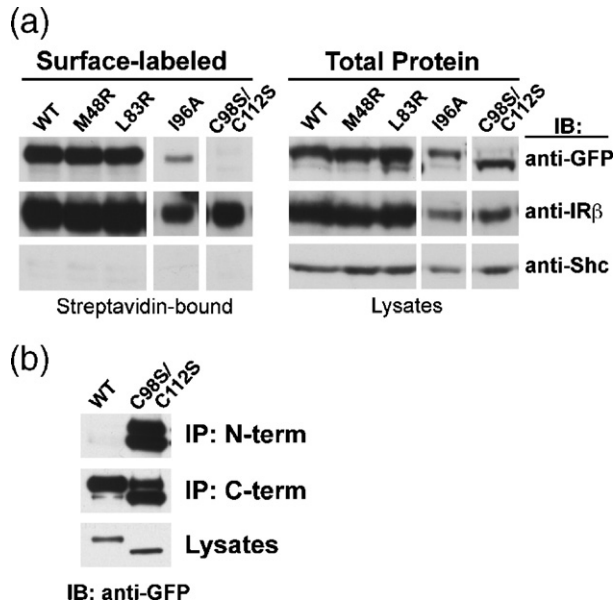


Figure 3. Surface expression of MuSK mutants. (a) MuSK M48R, L83R, and I96A, but not C98S/C112S, are expressed on the muscle cell surface. MuSK-GFP (wild-type or mutant) was stably expressed in cultured MuSK^{-/-} myotubes. Cell-surface proteins were labeled with membrane-impermeable NHS-biotin and captured with streptavidin-agarose beads. Clarified lysates (2% total loaded) and surface-labeled (streptavidin-bound; 50% bound loaded) proteins were resolved by SDS-PAGE and immunoblotted (IB) with antibodies to GFP to assess the presence of MuSK in the surface fraction (anti-GFP). Immunoblotting (IB) with antibodies to the insulin receptor β subunit (IR β) and Shc (66 kDa isoform shown) confirms that cell surface proteins are effectively labeled, while cytosolic proteins remain mostly in the unlabeled fraction. The lower protein level in all I96A samples is due to fewer myotubes used as starting material. (b) Extra disulfide on MuSK Ig1 is required for proper folding and processing of MuSK. NIH-3T3 cells stably expressing wild-type or C98S/C112S mutant MuSK-GFP were lysed. MuSK immunoprecipitation (IP) was performed using polyclonal antibodies against the N terminus (N-term) and the C terminus (C-term). GFP-tagged MuSK was detected by immunoblotting (IB) with an anti-GFP antibody.

analysis in the denaturing conditions of SDS-PAGE. This result suggests that the N-terminal epitope, which is otherwise masked in the properly folded, wild-type Ig1, is exposed when the extra disulfide bridge is not present. Taken together, these data indicate that the additional disulfide bridge is required for the proper folding of MuSK Ig1. This contrasts with the surface-exposed disulfide bridge in TrkA, which is not required for the structural integrity of Ig-like domain-5.²⁹

Met48, Leu83, and Ile96 are critical for agrin-induced MuSK activation

Proximal to the external disulfide bridge on Ig1 is Ile96 in β F (Figure 2(c), right), which occupies a

solvent-exposed position that is typically occupied by a hydrophilic residue in other Ig-like domains (e.g. Asn227 in FGF receptor-1, Figure 1(c)). Hydrophobic residues clustered near the external disulfide bridge in TrkA contribute to ligand (NGF) binding.²⁷ To test whether Ile96 is involved in agrin-induced MuSK activation, we generated an alanine point mutation at Ile96 in MuSK-GFP, and stably expressed the mutant receptor in MuSK^{-/-} muscle cells. Figure 3(a) shows that, unlike the double cysteine mutant, the MuSK I96A mutant receptor is expressed on the surface of muscle cells. Moreover, Ig1 in the I96A mutant is evidently folded properly, since the antibody to the N-terminal β strand of Ig1 was not able to immunoprecipitate the mutant receptor from myotube lysates (data not shown).

To test whether MuSK I96A is capable of being activated by agrin, we treated MuSK^{-/-} myotubes stably expressing wild-type or mutant MuSK-GFP with recombinant neural agrin, immunoprecipitated MuSK, and probed for receptor activation by blotting with an anti-phosphotyrosine antibody. Figure 4(a) shows that, while agrin induces activation of wild-type MuSK in a dose-dependent manner, activation of MuSK I96A is abolished completely.

Residues Met48 and Leu83 in MuSK Ig1 are at the center of the non-crystallographic dimer interface (Figure 2(b)). To begin to elucidate the function of this hydrophobic patch, we generated arginine point mutations at Met48 and Leu83 in MuSK-GFP, and stably expressed the mutants in MuSK^{-/-} muscle cells. As shown in Figure 3(a), the mutants are expressed on the surface of muscle cells at levels

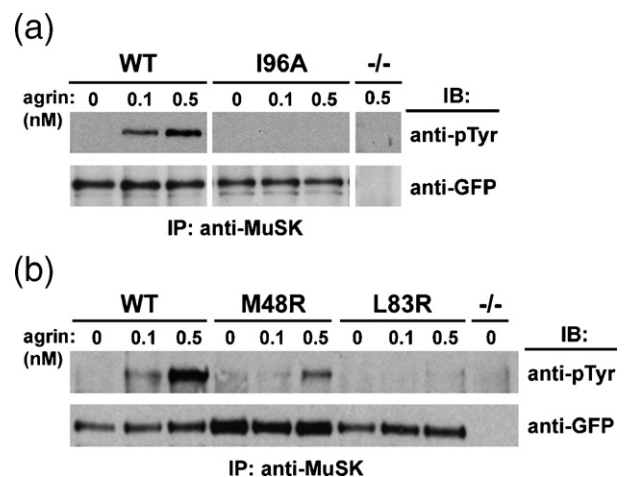


Figure 4. Mutations in MuSK Ig1 affect agrin-induced receptor activation. (a) Ile96 and (b) Met48 and Leu83 are required for agrin-induced activation. MuSK^{-/-} myotubes stably expressing MuSK-GFP (wild-type or mutant) were stimulated with 0.1 nM or 0.5 nM neural agrin for 30 min followed by MuSK immunoprecipitation (IP) with the C-terminal anti-MuSK antibody. IP samples were resolved by SDS-PAGE and immunoblotted (IB) with an anti-phosphotyrosine antibody (anti-pTyr) to assess MuSK activation. Blotting a duplicate membrane with anti-GFP antibody shows the relative level of MuSK-GFP in each sample.

equal to wild type. Furthermore, mutation of Met48 or Leu83 to arginine does not cause misfolding of Ig1, as neither mutant receptor is immunoprecipitated from myotube lysates by the N-terminal β strand antibody (data not shown).

To test the ability of MuSK M48R and L83R to be activated by agrin, we treated MuSK^{-/-} myotubes expressing wild-type or mutant MuSK-GFP with recombinant neural agrin, immunoprecipitated MuSK, and probed Western blots with anti-phosphotyrosine antibody. Figure 4(b) (top blot) shows that the level of activation of the mutant receptors M48R and L83R is reduced considerably compared to the robust activation of wild-type MuSK. The decrease in agrin-induced activation of the mutant receptors occurs despite the elevated expression levels of the mutants *versus* wild-type MuSK, as assessed by probing with antibodies against GFP (Figure 4(b), bottom blot). The stronger phosphotyrosine signal of MuSK M48R *versus* L83R with 0.5 nM agrin treatment is due to a greater amount of MuSK-GFP M48R in the myotubes. Quantitative densitometry analysis of the anti-phosphotyrosine and anti-GFP immunoblots indicates that the two mutants are equally unresponsive to agrin.

On the cell surface, we anticipate that the hydrophobic patch on Ig1 will mediate a protein-protein interaction, either MuSK homodimerization (as observed in the crystal structure) or a heterotypic interaction with another protein, such as agrin or a putative agrin co-receptor.⁵ One possible scenario is that the MuSK Ig1-2 dimer in the crystal structure represents a preformed, autoinhibited conformation of the receptor. There is evidence that some cytokine receptors (e.g. erythropoietin receptor) and RTKs (e.g. epidermal growth factor receptor) exist on the cell surface as inactive dimers and undergo ligand-induced rearrangements to form an active signaling complex.^{30,31} It is unlikely that the Ig1-mediated MuSK dimer observed in the crystal structure is autoinhibitory, since we did not observe an increase in the basal level of tyrosine phosphorylation in the dimer-disrupting M48R and L83R mutants (Figure 4(b)).

Another possibility is that the Ig1-mediated MuSK homodimer in the crystal structure reflects an active dimeric state whose formation is induced by agrin binding. We attempted cross-linking experiments in myotubes to assay agrin binding to wild-type MuSK and to MuSK M48R and L83R. However, even with wild-type MuSK, we were unable to detect a cross-linked agrin-MuSK complex (data not shown). Therefore, we are unable to distinguish whether Met48 and Leu83 in the Ig1 hydrophobic patch are critical for MuSK dimerization or for binding of agrin or a putative co-receptor. Nevertheless, to our knowledge, this is the first time that individual residues in the MuSK ectodomain have been identified as critical for agrin-stimulated MuSK activation. A greater understanding of the full componentry of the agrin-MuSK signaling complex will be required to fully elucidate the mechanisms of activation for this ligand-receptor pair.

Materials and Methods

Cell culture

Sf9 cells were maintained in EX-CELL 401 medium with L-glutamine (SAFC Biosciences) supplemented with 5% (v/v) fetal bovine serum (FBS), 0.1% (v/v) Pluronic F-68 (Cellgro Mediatech), and antibiotic-antimycotic (pen-strep (10 U/ml of penicillin and 10 μ g/ml of streptomycin), 25 ng/ml of amphotericin B; Invitrogen) at 27 °C. BOSC23 packaging cells³² were grown in Dulbecco's modified Eagle's medium (DMEM) with 1 mM glutamine, 10% FBS and 50 μ g/ml of gentamycin. NIH-3T3 cells were grown in DMEM with 10% FBS, 1 mM glutamine, 100 U/ml of pen-strep and 50 μ g/ml of gentamycin. MuSK^{-/-} myoblasts³³ were grown at 33 °C in growth medium containing DMEM plus 1 mM glutamine, 10% FBS, 10% (v/v) horse serum, 50 μ g/ml of gentamycin, 0.5% (v/v) chick embryo extract (CEE; Accurate Chemical), and 20 U/ml of recombinant mouse interferon- γ (IFN- γ ; Sigma) on dishes coated with Matrigel (BD Biosciences). Myoblasts at 90% confluence were induced to differentiate into myotubes by switching to 39 °C in medium lacking INF- γ and CEE.

Antibodies

The polyclonal antibody to the C-terminal sequence of rat MuSK (residues 849–868) has been described.³⁴ For production of the polyclonal antibody to the N-terminal sequence of rat MuSK, a peptide corresponding to residues 20–39 (GTEKLPKAPVITTPLETVD) was coupled to key-hole limpet hemocyanin and injected into rabbits (Research Genetics). The phosphotyrosine mAb 4G10 and polyclonal anti-Shc antibody were purchased from Upstate. The monoclonal GFP antibody B-2 was purchased from Santa Cruz Biotechnology. The polyclonal antibody against the insulin receptor β subunit was purchased from Biosource International. Horseradish-peroxidase-conjugated secondary antibodies were purchased from Jackson ImmunoResearch Laboratories and Biosource International.

Protein expression and purification

A PCR-generated cDNA fragment encoding MuSK Ig1-2 (residues 22–212 of rat MuSK) was ligated into the baculovirus transfer vector pAcGP67-B (BD Biosciences Pharmingen) that was modified to contain an N-terminal His₆ tag (a gift from Dr K. Carraway, UC Davis). Recombinant baculovirus was generated by co-transfecting Sf9 cells with transfer vector and linearized Baculo-Gold DNA according to the manufacturer's protocol (BD Biosciences Pharmingen). Adherent Sf9 cells were infected during log phase growth with high titer baculovirus, and media containing the secreted protein was harvested by centrifugation 72 h later. Secreted MuSK Ig1-2 protein, which is not glycosylated, was purified by nickel-affinity chromatography (His-Select HC; Sigma), gel-filtration chromatography (Superdex 75; GE Healthcare) and cation-exchange chromatography (Source S; GE Healthcare). Matrix-assisted laser desorption/ionization time-of-flight (MAL-DI-TOF) mass spectrometric analysis of purified MuSK Ig1-2 revealed a heterogeneous protein sample, due to *in vitro* proteolytic trimming. To obtain a homogeneous minimal protein fragment, MuSK Ig1-2 was subjected to limited proteolysis by trypsin (sequencing grade; Roche), which resulted in removal of 14 residues from the N terminus including the His₆-tag, leaving the

full Ig1-2 protein core intact. The sample was further purified over a Benzamidine HiTrap column (GE Healthcare) to remove trypsin, and cation-exchange chromatography (Source S) to obtain a homogeneous sample, as monitored by MALDI-TOF mass spectrometry, suitable for crystallization. Purified protein was concentrated in a spin concentrator (VivaScience).

Crystallization and data collection

Crystals of MuSK Ig1-2 were grown at 4 °C in hanging drops containing a 1:1 (v/v) ratio of protein solution at 9 mg/ml and reservoir buffer containing 8% (w/v) polyethylene glycol (PEG) 4000, 100 mM sodium acetate (pH 4.6), and 200 mM ammonium sulfate. (The same crystal form could be obtained at neutral pH, but the crystals were of poorer quality.) Crystals belong to orthorhombic space group $P2_12_12$ with unit cell dimensions $a=77.6$ Å, $b=118.0$ Å, and $c=57.8$ Å. There are two Ig1-2 molecules in the asymmetric unit with a solvent content of 61%. Before stream freezing in liquid nitrogen, crystals were equilibrated in a series of cryosolvents containing 5% (v/v), 10%, 15%, then 20%, ethylene glycol. A 2.2 Å dataset was collected on beamline X4A at the National Synchrotron Light Source, Brookhaven National Laboratory. Data were processed using DENZO/Scalepack.³⁵ A molecular replacement solution was found with AMoRE³⁶ with SWISS-MODEL homology models³⁷ of MuSK Ig1 and Ig2 based on the structure of telokin (PDB code 1FHG).²⁰ Rigid-body refinement, simulated annealing, and positional and B-factor refinement were performed with CNS³⁸ and Refmac,³⁹ and O⁴⁰ was used for model building.

Retroviral expression constructs and infection of cells

The SmaI/NotI fragment of pEGFP-N1 (Clontech) containing GFP cDNA was fused in-frame to the 3' end of full-length wild-type rat MuSK cDNA. MuSK-GFP cDNA was ligated into the pUC18 vector (Stratagene), where amino acid substitutions in the MuSK extracellular domain were generated by site-directed mutagenesis (QuikChange; Stratagene). All mutations were verified by automated DNA sequencing. The MuSK-GFP wild-type or mutant fragments were then ligated into the EcoRI site of the retroviral vector pBabe/puro.⁴¹ Full-length wild-type or mutant MuSK-GFP was stably expressed in NIH-3T3 and MuSK^{-/-} cells by retroviral infection. BOSC23 packaging cells were transfected with MuSK/GFP-pBabe/puro plasmids by the calcium phosphate precipitation method. Retrovirus-containing medium was collected two days post-transfection and used immediately for infection of NIH-3T3 and MuSK^{-/-} cells, or flash-frozen and stored at -80 °C. For infection, NIH-3T3 cells and MuSK^{-/-} myoblasts at 30–50% confluence were incubated with growth medium containing virus and 8 µg/ml of polybrene for 4 h. The concentration of polybrene was then diluted to 2 µg/ml by addition of growth medium, and cells were incubated overnight. At 24–48 h post-infection, cells were placed under selection with medium containing 4 µg/ml of puromycin and maintained under selective conditions until stable pools were formed.

MuSK activation by agrin and MuSK immunoprecipitation

For agrin-induced MuSK stimulation, fully differentiated myotubes were treated with 0.1–0.5 nM neural agrin (R&D Systems) in DMEM for 30–50 min at 37 °C. For all

MuSK immunoprecipitation experiments, myotubes or NIH-3T3 cells were rinsed twice with ice-cold phosphate-buffered saline (PBS) and lysed in lysis buffer containing 1% (v/v) NP-40, 30 mM triethanolamine (pH 7.5), 50 mM NaCl, 5 mM EDTA, 5 mM EGTA, 50 mM NaF, 2 mM sodium orthovanadate, 1 mM sodium tetrathionate, 1 mM N-ethylmaleimide, 10 µM of Pepstatin A, 0.5 mg/ml of Pefabloc (Roche), and a Complete protease inhibitor tablet (Roche). Whole-cell lysates were cleared by centrifugation, and MuSK protein was immunoprecipitated at 4 °C overnight with the N-terminal (Figure 4(b)) or the C-terminal (Figure 4(b) and (c)) anti-MuSK antibodies. The antibodies and bound proteins were captured by incubating with protein A-agarose beads (Roche) for an additional hour at 4 °C. The beads were then washed four times in freshly made lysis buffer. Bound proteins were eluted with Laemmli sample buffer, resolved by SDS-PAGE, and transferred to polyvinylidene difluoride membrane (PVDF, Millipore). Membranes were blocked in Tris-buffered saline containing 0.05% Tween-20 and 5% bovine serum albumin (BSA; for anti-phosphotyrosine blots) or 5% instant skimmed milk, and probed with primary antibodies and horseradish peroxidase-conjugated secondary antibodies, which were visualized with SuperSignal West Pico and West Femto Substrates (Pierce).

Biotinylation of cell surface proteins

Myotubes were washed extensively with PBS/Ca/Mg (PBS containing 0.1 mM CaCl₂ and 1 mM MgCl₂) and incubated with 1 mM EZ-link sulfo-NHS-LC-biotin (Pierce) in PBS/Ca/Mg at room temperature for 30 min. The reaction was quenched by rinsing the cells twice with PBS/Ca/Mg containing 100 mM glycine, then incubating in DMEM at 37 °C for 30 min. The cells were then placed on ice, washed with ice-cold PBS, and lysed in RIPA buffer (1% (v/v) NP-40, 1% (w/v) sodium deoxycholate, 150 mM NaCl, 10 mM sodium phosphate buffer (pH 7.2), 2 mM EDTA, 50 mM NaF, 2 mM sodium orthovanadate, 10 µM Pepstatin A, 0.5 mg/ml of Pefabloc, and a Complete protease inhibitor tablet (Roche) containing 0.5% (w/v) SDS. Lysates were cleared by centrifugation, and biotin-labeled proteins were recovered by incubating with streptavidin-agarose (Sigma) for 4 h at 4 °C, followed by four washes with RIPA buffer containing 0.1% SDS. Proteins bound to streptavidin-agarose were eluted with Laemmli sample buffer, and bound and total proteins were resolved by SDS-PAGE and detected by Western blotting.

Data accession numbers

The coordinates and structure factors for the MuSK Ig1-2 crystal structure have been deposited in the Protein Data Bank with accession number 2IEP.

Acknowledgements

Support from the National Institutes of Health (NS053414 to S.R.H., NS036193 to S.J.B.) is acknowledged. We thank M Mohammadi for helpful comments on the manuscript, G. Dorsainville and M. Frieser for experimental support and discussions,

R. Abramowitz for synchrotron data collection assistance, and Dr K. Carraway for the baculovirus transfer vector.

References

- Burden, S. J. (2002). Building the vertebrate neuromuscular synapse. *J. Neurobiol.* **53**, 501–511.
- McMahan, U. J. (1990). The agrin hypothesis. *Cold Spring Harbor Symp Quant. Biol.* **55**, 407–418.
- Jennings, C. G., Dyer, S. M. & Burden, S. J. (1993). Muscle-specific trk-related receptor with a kringle domain defines a distinct class of receptor tyrosine kinases. *Proc. Natl Acad. Sci. USA*, **90**, 2895–2899.
- Valenzuela, D. M., Stitt, T. N., DiStefano, P. S., Rojas, E., Mattsson, K., Compton, D. L. *et al.* (1995). Receptor tyrosine kinase specific for the skeletal muscle lineage: expression in embryonic muscle, at the neuromuscular junction, and after injury. *Neuron*, **15**, 573–584.
- Glass, D. J., Bowen, D. C., Stitt, T. N., Radziejewski, C., Bruno, J., Ryan, T. E. *et al.* (1996). Agrin acts via a MuSK receptor complex. *Cell*, **85**, 513–523.
- Gautam, M., Noakes, P. G., Moscoso, L., Rupp, F., Scheller, R. H., Merlie, J. P. *et al.* (1996). Defective neuromuscular synaptogenesis in agrin-deficient mutant mice. *Cell*, **85**, 525–535.
- DeChiara, T. M., Bowen, D. C., Valenzuela, D. M., Simmons, M. V., Poueymirou, W. T., Thomas, S. *et al.* (1996). The receptor tyrosine kinase MuSK is required for neuromuscular junction formation in vivo. *Cell*, **85**, 501–512.
- Hopf, C. & Hoch, W. (1998). Tyrosine phosphorylation of the muscle-specific kinase is exclusively induced by acetylcholine receptor-aggregating agrin fragments. *Eur. J. Biochem.* **253**, 382–389.
- Ullrich, A. & Schlessinger, J. (1990). Signal transduction by receptors with tyrosine kinase activity. *Cell*, **61**, 203–212.
- Hubbard, S. R. & Till, J. H. (2000). Protein tyrosine kinase structure and function. *Annu. Rev. Biochem.* **69**, 373–398.
- Glass, D. J., Apel, E. D., Shah, S., Bowen, D. C., DeChiara, T. M., Stitt, T. N. *et al.* (1997). Kinase domain of the muscle-specific receptor tyrosine kinase (MuSK) is sufficient for phosphorylation but not clustering of acetylcholine receptors: required role for the MuSK ectodomain? *Proc. Natl Acad. Sci. USA*, **94**, 8848–8853.
- Xu, Y. K. & Nusse, R. (1998). The Frizzled CRD domain is conserved in diverse proteins including several receptor tyrosine kinases. *Curr. Biol.* **8**, R405–R406.
- Rehn, M., Pihlajaniemi, T., Hofmann, K. & Bucher, P. (1998). The frizzled motif: in how many different protein families does it occur? *Trends Biochem Sci.* **23**, 415–417.
- Wiesmann, C., Muller, Y. A. & de Vos, A. M. (2000). Ligand-binding sites in Ig-like domains of receptor tyrosine kinases. *J. Mol. Med.* **78**, 247–260.
- Zhou, H., Glass, D. J., Yancopoulos, G. D. & Sanes, J. R. (1999). Distinct domains of MuSK mediate its abilities to induce and to associate with postsynaptic specializations. *J. Cell Biol.* **146**, 1133–1146.
- Cornish, T., Chi, J., Johnson, S., Lu, Y. & Campanelli, J. T. (1999). Globular domains of agrin are functional units that collaborate to induce acetylcholine receptor clustering. *J. Cell. Sci.* **112**, 1213–1223.
- Gesemann, M., Denzer, A. J. & Ruegg, M. A. (1995). Acetylcholine receptor-aggregating activity of agrin isoforms and mapping of the active site. *J. Cell Biol.* **128**, 625–636.
- Hoch, W., Campanelli, J. T., Harrison, S. & Scheller, R. H. (1994). Structural domains of agrin required for clustering of nicotinic acetylcholine receptors. *EMBO J.* **13**, 2814–2821.
- Harpaz, Y. & Chothia, C. (1994). Many of the immunoglobulin superfamily domains in cell adhesion molecules and surface receptors belong to a new structural set which is close to that containing variable domains. *J. Mol. Biol.* **238**, 528–539.
- Holden, H. M., Ito, M., Hartshorne, D. J. & Rayment, I. (1992). X-ray structure determination of telokin, the C-terminal domain of myosin light chain kinase, at 2.8 Å resolution. *J. Mol. Biol.* **227**, 840–851.
- Freigang, J., Proba, K., Leder, L., Diederichs, K., Sonderegger, P. & Welte, W. (2000). The crystal structure of the ligand binding module of axonin-1/TAG-1 suggests a zipper mechanism for neural cell adhesion. *Cell*, **101**, 425–433.
- Bazan, J. F. (1990). Structural design and molecular evolution of a cytokine receptor superfamily. *Proc. Natl Acad. Sci. USA*, **87**, 6934–6938.
- Muller, Y. A., Ultsch, M. H. & de Vos, A. M. (1996). The crystal structure of the extracellular domain of human tissue factor refined to 1.7 Å resolution. *J. Mol. Biol.* **256**, 144–159.
- Walter, M. R., Windsor, W. T., Nagabhushan, T. L., Lundell, D. J., Lunn, C. A., Zauodny, P. J. & Narula, S. K. (1995). Crystal structure of a complex between interferon-gamma and its soluble high-affinity receptor. *Nature*, **376**, 230–235.
- Kuehn, R., Eckler, S. A. & Gautam, M. (2005). Multiple alternatively spliced transcripts of the receptor tyrosine kinase MuSK are expressed in muscle. *Gene*, **360**, 83–91.
- Lawrence, M. C. & Colman, P. M. (1993). Shape complementarity at protein/protein interfaces. *J. Mol. Biol.* **234**, 946–950.
- Wiesmann, C., Ultsch, M. H., Bass, S. H. & de Vos, A. M. (1999). Crystal structure of nerve growth factor in complex with the ligand-binding domain of the TrkA receptor. *Nature*, **401**, 184–188.
- Watty, A. & Burden, S. J. (2002). MuSK glycosylation restrains MuSK activation and acetylcholine receptor clustering. *J. Biol. Chem.* **277**, 50457–50462.
- Urfer, R., Tsoulfas, P., O'Connell, L., Hongo, J. A., Zhao, W. & Presta, L. G. (1998). High resolution mapping of the binding site of TrkA for nerve growth factor and TrkC for neurotrophin-3 on the second immunoglobulin-like domain of the Trk receptors. *J. Biol. Chem.* **273**, 5829–5840.
- Livnah, O., Stura, E. A., Middleton, S. A., Johnson, D. L., Jolliffe, L. K. & Wilson, I. A. (1999). Crystallographic evidence for preformed dimers of erythropoietin receptor before ligand activation. *Science*, **283**, 987–990.
- Moriki, T., Maruyama, H. & Maruyama, I. N. (2001). Activation of preformed EGF receptor dimers by ligand-induced rotation of the transmembrane domain. *J. Mol. Biol.* **311**, 1011–1026.
- Pear, W. S., Nolan, G. P., Scott, M. L. & Baltimore, D. (1993). Production of high-titer helper-free retroviruses by transient transfection. *Proc. Natl Acad. Sci. USA*, **90**, 8392–8396.
- Herbst, R. & Burden, S. J. (2000). The juxtamembrane region of MuSK has a critical role in agrin-mediated signaling. *EMBO J.* **19**, 67–77.

34. Watty, A., Neubauer, G., Dreger, M., Zimmer, M., Wilm, M. & Burden, S. J. (2000). The in vitro and in vivo phosphotyrosine map of activated MuSK. *Proc. Natl Acad. Sci. USA*, **97**, 4585–4590.
35. Otwinowski, Z. & Minor, W. (1997). Processing of X-ray diffraction data collected in oscillation mode. *Methods Enzymol.* **276**, 307–326.
36. Navaza, J. (1994). AMoRe: an automated package for molecular replacement. *Acta Crystallog. sect. A*, **50**, 157–163.
37. Peitsch, M. C. (1996). ProMod and Swiss-Model: internet-based tools for automated comparative protein modelling. *Biochem. Soc. Trans.* **24**, 274–279.
38. Brunger, A. T., Adams, P. D., Clore, G. M., DeLano, W. L., Gros, P., Grosse-Kunstleve, R. W. *et al.* (1998). Crystallography & NMR system: a new software suite for macromolecular structure determination. *Acta Crystallog. sect. D*, **54**, 905–921.
39. Murshudov, G. N., Vagin, A. A. & Dodson, E. J. (1997). Refinement of macromolecular structures by the maximum-likelihood method. *Acta Crystallog. sect. D*, **53**, 240–255.
40. Jones, T. A., Zou, J. Y., Cowan, S. W. & Kjeldgaard, M. (1991). Improved methods for building protein models in electron density maps and the location of errors in these models. *Acta Crystallog. sect. A*, **47**, 110–119.
41. Morgenstern, J. P. & Land, H. (1990). Advanced mammalian gene transfer: high titre retroviral vectors with multiple drug selection markers and a complementary helper-free packaging cell line. *Nucl. Acids Res.* **18**, 3587–3596.
42. Plotnikov, A. N., Schlessinger, J., Hubbard, S. R. & Mohammadi, M. (1999). Structural basis for FGF receptor dimerization and activation. *Cell*, **98**, 641–650.
43. Holm, L. & Sander, C. (1996). Alignment of three-dimensional protein structures: network server for database searching. *Methods Enzymol.* **266**, 653–662.
44. Laskowski, R. A., MacArthur, M. W., Moss, D. S. & Thornton, J. M. (1993). PROCHECK: a program to check the stereochemical quality of protein structures. *J. Appl. Crystallog.* **26**, 283–291.
45. Nicholls, A., Sharp, K. A. & Honig, B. (1991). Protein folding and association: insights from the interfacial and thermodynamic properties of hydrocarbons. *Proteins: Struct. Funct. Genet.* **11**, 281–296.

Edited by I. Wilson

(Received 13 June 2006; received in revised form 30 August 2006; accepted 5 September 2006)
Available online 12 September 2006